Enhanced Pulse Compression within Sign-Alternating Dispersion Waveguides: supplemental document

Haider Zia

University of Twente, Department Science & Technology, Laser Physics and Nonlinear Optics Group, MESA+ Research Institute for Nanotechnology, Enschede 7500 AE, The Netherlands

1. Negligible Impact of Self-Steepening and Raman Effect

The Raman effect for femtosecond pulses becomes the instantaneous electronic effect, because the delayed response from the material response function is 10's of ps and is thus out of the frame of the pulse of concern [1].

The simulation already accounts for the instantaneous Raman effect by the approximation used in main paper reference 1. That is to reduce the nonlinear waveguide coefficient (by a factor $1-0.18$).

The Raman effect can be totally neglected for SiN waveguides at a pulse wavelength in the IR, for femtosecond pulses [2], however, we stick with the approximation given in reference 1 for this case as well.

We recently found that for the fiber case, a better estimate based on experimentation is given as a reduction in the nonlinear coefficient by subtracting $0.8\ \mathrm{E}-3\ (\mathrm{W}^{-1}\mathrm{m}^{-1})$, found in [3]; thus, the nonlinear waveguide coefficient becomes $4.4\ \mathrm{E}\ -3\ (\mathrm{W}^{-1}\mathrm{m}^{-1})$ instead of $5.2\ \mathrm{E}\ -3\ (\mathrm{W}^{-1}\mathrm{m}^{-1})$. We put this new parameter in our simulator to see if the results change.

In addition, we included self-steepening, following the procedure outlined in the main text [1]. Here the coefficient for self-steepening is given as $0.05\ \mathrm{E}\ -3\ (\mathrm{W}^{-1}\mathrm{m}^{-1})$ (with the normalized time coordinate used in the simulation) for the fiber case is approx. a factor of 100 less than the SPM coefficient in the fiber and integrated SiN waveguide case.

To prove that the above effects are negligible, we numerically show the results of the final normalized power profile versus normalized pulse time (normalized to 72 fs) in the frame of reference of the pulse at the exit of the fiber with inclusion of both the new Raman correction and self-steepening (red curve) compared to the old value without these corrections, shown in Fig. 1a. As can be seen, the two power profiles are virtually indistinguishable and the 1/e duration values differ only negligibly. The same parameters and length were used as in the main paper for section 3.1.

The spectral energy density of the two cases (with the same color code as Fig. 1a) versus normalized frequency (0 frequency corresponds to the freq. of the central wavelength 1.55um) is given in Fig. 1b. Here too, the curves are negligibly distinguishable with nearly the same 1/e bandwidth. The same parameters and length were used as in Fig. 1a (and the main paper).

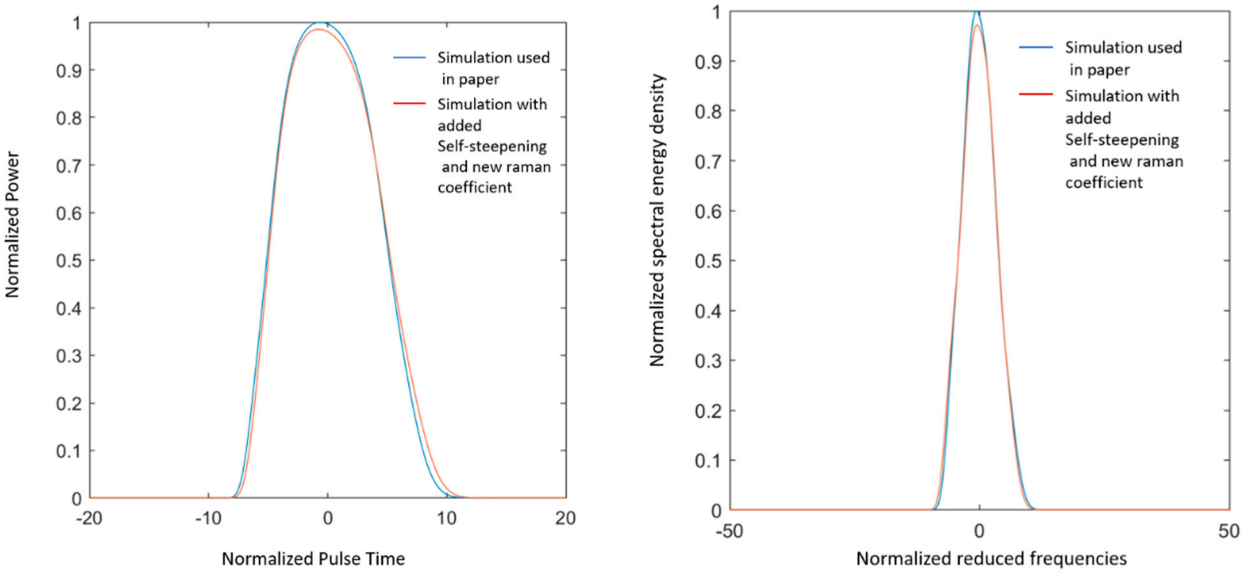

a) b)

Figure 1. a) Normalized power profile of the pulse exiting the ND fiber with and without new Raman gain efficiency coefficient and self-steepening effect. b) Normalized spectral energy density of the pulse exiting the fiber with and without mentioned effects. The same parameters and length were used as in the main paper.

This numerical example supports the conclusion that the self-steepening and Raman terms can be turned off to focus on the SPM–dispersion interaction, without loss of generality.

2. Proof of Eq. 1

From the condition $\tau_2 \approx \tau_1$ and the phase function of the illustrative pulse at location z, in Fig. 2, given as $\varphi_1 = \frac{\beta_2}{2}\nu^2 + \frac{\beta_3}{6}\nu^3$, it can be shown that,

$$\frac{d\varphi_2\left(\frac{\nu_2}{\nu_1}\nu\right)}{d\nu} \approx \frac{d\varphi_1}{d\nu} \tag{S1a}$$

for the phase function for the pulse at location $z + \Delta z$.

Therefore,

$$\varphi_2 = \frac{\beta_{2\prime}}{2}\nu^2 + \frac{\beta_{3\prime}}{6}\nu^3 \tag{S1b}$$

where,

$$\beta_{2\prime} \approx \frac{\nu_1}{\nu_2}\beta_2$$

$$\beta_{3\prime} \approx \left(\frac{\nu_1}{\nu_2}\right)^2 \beta_3 \qquad \text{(main text Eq. 1)}$$

ending the proof.

3. Derivation of Main Text Eq. 3 and Peak of β_2 Explanation

The emergence of the peak of β_2 is physically explained by two competing quantities, i.e., the increasing difference between the actual pulse duration, τ, and the transform-limited duration, τ_{lim}, labeled as $\Delta T = \tau - \tau_{lim}$ as a function of propagation, and the bandwidth increase. With increasing ΔT, the spectral phase coefficient must increase to stretch the pulse in time. However, the bandwidth increase reduces the spectral phase coefficient. At the beginning ΔT increases much more rapidly than the bandwidth increase, but then saturates as τ_{lim} asymptotically approaches zero. Thus, after the peak in the spectral coefficient, the increasing bandwidth reduces the coefficient.

To explain why β_2 increases to a peak value, we relate pulse duration to the second-order spectral phase coefficient. We consider that the pulse's duration is affected predominantly only by the overall second-order phase at this beginning region of propagation. The second-order phase approximation is valid in this beginning region since second-order dispersion dominates over higher-orders and the pulse remains Gaussian, so SPM predominantly also adds second-order spectral phase as well (especially within the 1/e bandwidth). Thus, by using the equation for second-order dispersive temporal propagation of a Gaussian pulse [22] the behavior seen in Fig. 3a is explained quite well. The representative equation is given as,

$$\tau = \sqrt{1 + \left(4\frac{\beta_2}{{\tau_{lim}}^2}\right)^2}\,\tau_{lim} \tag{S2}$$

where $\tau_{lim} = \frac{4}{\Delta\nu}$ is the transform-limited duration. Rearranging Eq. S2 for β_2 then yields,

$$\beta_2 = \frac{1}{4}\left[\sqrt{\left(\frac{\tau}{\tau_{lim}}\right)^2 - 1}\right]{\tau_{lim}}^2 \tag{S3}$$

which maximizes when $\tau_{lim} = \frac{\tau}{\sqrt{2}}$, or in terms of bandwidth, when $\tau \approx 4\sqrt{2}/\Delta\nu$, which occurs when the peak of Figure 4, curve a, is reached. For further pulse propagation past the peak of the second-order spectral phase coefficient, τ is always greater than $4\sqrt{2}/\Delta\nu$, since τ and $\Delta\nu$ continually increase with propagation.

While main text equation 3 is also the limit of Eq. S3 for propagation past the peak of β_2, we derive main text equation 3 under the influence of the full higher order dispersion, now present as the propagation distance has increased. When, $\tau > 4\sqrt{2}/\Delta\nu$, the approximation can be made that,

$$\tau = 2\frac{d\varphi}{d\nu}\bigg|_{\frac{\Delta\nu}{2}} = \sum_{n=2}^{\infty}\frac{2}{n-1!}\frac{d^n\varphi}{d\nu^n}\bigg|_{\nu_o}\left(\frac{\Delta\nu}{2}\right)^{n-1} \tag{S4}$$

Rearranging for β_2, we arrive at:

$$\beta_2 = \frac{\tau}{\Delta\nu} - \sum_{n=3}^{\infty}\frac{1}{n-1!}\frac{d^n\varphi}{d\nu^n}\bigg|_{\nu_o}\left(\frac{\Delta\nu}{2}\right)^{n-2} \tag{S5}$$

Equation S5 is always greater than zero, therefore, at most β_2 scales as

$$\beta_2(\Delta z) \propto \frac{\tau(\Delta z)}{\Delta\nu(\Delta z)}.$$

4. Derivation of Main Text Equation 4

By rearranging Eq. S4, for β_3, it is seen that β_3 scales at most with the bandwidth like,

$$|\beta_3(\Delta z)| \propto \frac{\tau(\Delta z))}{\Delta\nu(\Delta z)^2}$$

An adjustment to the proof shown in Eq. S4 -S5 in the Supplementary Materials, must be made for odd-order coefficients (e.g., 3rd order) because they follow the same sign as the same-order waveguide GVD coefficient and could be negative (e.g., the numerical example of Fig. 2 main text). This means that the summation term of Eq. S4 is not smaller than τ. However, for odd-orders, it can still be proven that, at most, $|\beta_n(\Delta z)| \propto \frac{\tau(\Delta z)}{\Delta\nu(\Delta z)^{n-1}}$. First, $|\beta_n(\Delta z)| \propto \frac{\tau_n(\Delta z)}{\Delta\nu(\Delta z)^{n-1}}$, where $\tau_n(\Delta z) = \left|\tau_{1/e} - |\tau_{-1/e}|\,\right|$ and $\tau_{\pm 1/e}$ are the time values of the 1/e values. However, $\left|\tau_{1/e} - |\tau_{-1/e}|\,\right| \le \tau = \tau_{1/e} + |\tau_{-1/e}|$. Therefore, odd-coefficients scale still in a maximal manner as $|\beta_n(\Delta z)| \propto \frac{\tau(\Delta z)}{\Delta\nu(\Delta z)^{n-1}}$.

For even-order coefficients, they are always positive because SPM generates bluer frequencies on the trailing side of the pulse and redder frequencies on the leading side of the pulse. Since the pulse is spreading in time due to the dominant ND β_2, this enforces that all even higher-order coefficients are positive.

Higher-order self-phase modulation, such as self-steepening only contributes to additional bandwidth development and thus contributes to the reduction in the third-order and higher order phase coefficients. The asymmetric temporal profile that develops because of self-steepening, will not impede the reduction in phase coefficients; instead, it would contribute to a non-symmetric horizontal scaling of the spectral phase function. It can be shown that this weighted horizontal scaling reduces the phase coefficients as shown in the main text equations, but adds as well a small higher order phase contribution (for example, 4th order) to the order being considered in the analysis. However, this contribution then reduces over the propagation by the same processes as discussed in the main text. Therefore, it is expected that overall, self-steepening accelerates the phase coefficient reduction over propagation.

5. General Method for Obtaining any AD GVD

In this appendix we derive a general method for obtaining any needed AD GVD such that the pulse obtains a transform-limited duration at the end of the segment. These results are not only applicable to sign-alternating dispersion SCG waveguides but for general nonlinear pulse compression schemes.

We proceed by splitting the AD segment into several sub-segments, for the goal of compensating the spectral phase of the pulse coming out of the ND segment. The overall GVD coefficient of these sub-segments is anomalous to compensate for the positive second-order spectral phase coefficient of the pulse exiting the ND segment. The number of such sub-segments, labeled as n, determines the order precision of spectral phase compensation. For example, two sub-segments would compensate up to the third-order spectral phase; three would compensate up to fourth-order and so forth. We show this AD segment scheme in Fig. S2.

Next, for an optical pulse having traversed these sub-segments, perfect spectral phase compensation up to order "$n+1$" would be achieved if the segments satisfy:

$$\begin{gathered} -\sum_{k=1}^{n} d_{2,k} L_k = \beta_2 \\ -\sum_{k=1}^{n} d_{3,k} L_k = \beta_3 \\ -\sum_{k=1}^{n} d_{n+1,k} L_k = \beta_n \end{gathered} \tag{S6}$$

where, $d_{j,k}$ is the j^{th} dispersion coefficient (taken about ν_o) of a sub-segment indexed by the number k. L_k is the length of the specific sub-segment.

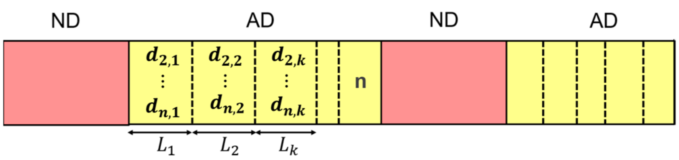

Figure 2. AD segments are split into sub-segments, where the sub-segment dispersion coefficients satisfy (A1).

We represent Equation A1 in the more convenient matrix form,

$$\mathbf{A}\mathbf{x} = \mathbf{y} \tag{S7}$$

Where, $\mathbf{A}$ is an n by k matrix formed with the d's as elements, i.e., $d_{j,k}$ (rows labeled by index j, columns by index k). $\mathbf{x}$ is a column vector of segment lengths, and $\mathbf{y}$ is the column vector of increasing the spectral phase derivatives of the pulse exiting the ND segment about ν_o. The physical constraint of the above system of equations is that the segment lengths must all be positive. We also note that normal dispersion segments could be used, since the sign of higher-order dispersion coefficients are not constrained to a particular choice (ND or AD), and thus they can be used for these higher-order $d_{j,k}$ in the above system of equations. A set of unique waveguide GVD's to enable the solution of (A1) could be found by varying the sub-segment geometrical cross-section (e.g., such as core radius in fiber).

Supplementary References

1. G. Fanjoux, S. Margueron, J.C. Beugnot, and T. Sylvestre, "Supercontinuum generation by stimulated Raman–Kerr scattering in a liquid-core optical fiber". JOSA B, 34(8), pp.1677-1683.
2. A. Klenner, A. S. Mayer, A. R. Johnson, K. Luke, M. R. E. Lamont, Y. Okawachi, M. Lipson, A. L. Gaeta, U. Keller, Opt. Express 2016, 24, 11043.